Talanta Open 7 (2023) 100223

Contents lists available at ScienceDirect

Talanta Open

journal homepage: www.sciencedirect.com/journal/talanta-open

A facile method for *in-situ* detection of thiabendazole residues in fruit and vegetable peels using Surface-Enhanced Raman Spectroscopy

María Luz Rizzato, A. Lorena Picone *, Rosana M. Romano *

CEQUINOR (UNLP, CCT-CONICET La Plata, associated with CIC-PBA), Departamento de Química, Facultad de Ciencias Exactas, Universidad Nacional de La Plata, Boulevard 120 N° 1465, La Plata, CP 1900, Argentina

ARTICLE INFO

Keywords:
Flexible SERS substrate
Pesticide residues
In-situ detection
Thiabendazole

ABSTRACT

A flexible Surface-Enhanced Raman Spectroscopy (SERS) substrate based on silver nanoparticles encapsulated in an agar gel has been probed to detect the fungicide thiabendazole (TBZ) reaching a limit of detection (LOD) of 30 ng/cm^2. In addition, a simple and sensitive strategy was employed for *in-situ* detection of TBZ on fruit and vegetable peels. For that purpose, peels of different fruits and vegetables were intentionally contaminated with different amount of TBZ, and the analyte was subsequently extracted within few seconds by gently rubbing the surface with the SERS substrate. The lowest value of TBZ detected on eggplant and green pepper peels was 50 ng/cm^2. The values achieved for apple and pear peels were 0.20 μg/cm^2 and 40 ng/cm^2, respectively. On the other hand, for tomato and strawberry peels the lowest value achieved was 0.50 μg/cm^2. The variation in sensitivity can be attributed to differences in the surface properties of the different peels. The above results show that this flexible SERS substrate can be further employed for the detection of contaminants in practical applications for food safety inspection.

1. Introduction

Food quality and safety have been gaining increasing attention in recent years, being essential the improvement in methods to detect, eliminate and control the risks posed by hazardous substances such as pesticides, adulterants, and other contaminants. Thiabendazole (TBZ) is a systemic benzimidazole fungicide used to control a variety of fruit and vegetable diseases such mold, blight, rot and stains caused by various fungi [1]. TBZ can be applied by dipping, spraying, or during the waxing procedure for fruits and vegetables. TBZ presents low acute toxicity to humans; however, the United Stated Environmental Protection Agency (U.S. EPA) has classified TBZ as likely carcinogenic at doses high enough to disrupt thyroid hormone balance [1]. People may be exposed to residues of TBZ through the diet; furthermore, maximum residue limits (MRL) have been established for numerous agricultural and livestock commodities. The U.S. EPA prescribes a MRL for TBZ of 10 ppm for citrus fruits and 12 ppm for apples (wet pomace) [2]. While in Argentina SENASA [3] (National Service of Sanitation and Agri-Food Quality) establishes a MRL of 10 ppm for citrus fruits and 3 ppm for apples. In the European Union, the European Commission [4] establishes a MRL of 7 ppm for citrus fruits and 4 ppm for apples and pears.

Surface-Enhanced Raman Spectroscopy (SERS) is a well-suited analytical tool for rapid, non-invasive and sensitive detection of different substances. In recent years, the development and application of innovative SERS methods has notary increased, especially those suitable for the detection of pesticides residues for food safety controls [5–7]. In this context, the development of flexible SERS substrates, as an alternative for *in-situ* analysis, have progressively attracted the scientific interest [8–12]. Recently, we have used a new flexible SERS substrate containing silver nanoparticles on an agar gel to detect thiram residues in fruit and vegetable peels [13]. The Ag NPs gel substrate possess the advantage of easy sampling by stamping the surface peels which facilitates the detection of contaminants present therein. Moreover, the substrate was also employed to detect the presence of cocaine in $100 Argentinian banknotes [14]. Herein, we report a rapid and sensitive method for the *in-situ* detection of TBZ residues in fruit and vegetable peels using the AgNPs gel substrate.

* Corresponding authors.
E-mail addresses: alpicone@quimica.unlp.edu.ar (A.L. Picone), romano@quimica.unlp.edu.ar (R.M. Romano).

https://doi.org/10.1016/j.talo.2023.100223
Received 25 January 2023; Received in revised form 1 April 2023; Accepted 24 April 2023
Available online 28 April 2023

2. Materials and methods

2.1. Chemicals and materials

Thiabendazole (2-(4-Thiazolyl)benzimidazole, $C_{10}H_7N_3S$, ≥ 99%, Merk, China), 4−mercaptobenzolic acid ($C_7H_6O_2S$, > 99%, Sigma-Aldrich, St Louis, USA), silver nitrate ($AgNO_3$, 99.0%, Cicarelli, USA), trisodium citrate dehydrate ($Na_3C_6H_5O_7.2H_2O$, 99.0%, Cicarelli, Spain), sodium borohydride ($NaBH_4$, ≥ 98.0%, Biopack, Buenos Aires, Argentina), methanol (Biopack, Buenos Aires, Argentina), ethanol (Soria, Buenos Aires, Argentina), acetone (Carlo Erba, Milan, Italy) and agar (Merk, Spain), were used as received. The silver nanoparticle dispersions were prepared using Milli-Q water (17.8 MΩ cm). A detailed description of the glassware cleaning was described in the Supporting Information. Grids for STEM (Scanning Transmition Electron Microscopy) measurements were purchased from Ted Pella INC., USA.

Fresh fruits and vegetables were acquired in local markets (La Plata, Buenos Aires, Argentina) and before being used in the laboratory tests were thoroughly washed first with tap water and subsequently with Milli-Q water. Fruits and vegetables peel pieces of approximately 1 cm^2 were contaminated by dropping TBZ solutions of different concentrations. Blank samples of each fruit or vegetable peel were also prepared by dropping only methanol on the surfaces.

2.2. SERS substrate fabrication and characterization

As mentioned above, the SERS substrate used in this study was an agar gel containing silver nanoparticles (Ag NPs gel substrate). The substrate preparation method and its more relevant characterization have been previously reported [13]. In summary, citrated-capped Ag NPs were synthesized using a procedure previously described by Isanova and Zamborini [15]. Later, the as-prepared Ag NPs dispersion was diluted 1:10 ratio with Milli-Q water and subsequently the UV-Vis spectrum was measured in order to check the obtained particles. STEM microscopy was used to examine the particles morphology. After that, the as-prepared Ag NPs dispersion was employed to fabricate the SERS substrates, following the general procedure proposed by Platania et al. [16]. The detailed preparation procedure is described in the Supporting Information. In order to examine the distribution of the Ag NPs in the agar gel STEM images of the dehydrated Ag NPs substrate were collected after coating the sample with a gold thin layer (~ 10 nm) to avoid charging effects.

2.3. Samples preparation and sampling procedures

4−mercaptobenzolic acid (4−MBA) was used as probing molecule to determine the enhancement factor of Ag NPs gel substrate as it is easily absorbed on the silver surface [17]. A stock solution of 4−MBA in ethanol (1.0×10^{-2} M) was prepared. Ethanol solutions of 4-MBA with different concentrations (1.0×10^{-3}; 1.0×10^{-4}; 1.0×10^{-5} and 1.0×10^{-7} M) were prepared from the stock solution. A concentrated solution of 4−MBA in acetone (0.16 M) was also prepared in order to measure the normal Raman spectrum of 4−MBA in solution as ethanol exhibits Raman signals than interfere with the main 4−MBA bands. On the other hand, a stock solution of TBZ in methanol (1.0×10^{-2} M) was daily prepared. Methanol solutions of TBZ with different concentrations (1.0×10^{-6}; 5.0×10^{-6}; 1.0×10^{-5}; 2.5×10^{-5}; 3.3×10^{-5}; 5.0×10^{-5}; 7.5×10^{-5}; 1.0×10^{-4}; 2.5×10^{-4}; 5.0×10^{-4}; 7.5×10^{-4}; 1.0×10^{-3} and 5.0×10^{-3} M) were prepared from the stock solution.

In order to investigate the possibility of resonance or pre-resonance Raman effects of the analyte, the UV-Vis spectra of solutions of thiabendazole in methanol were obtained prior to begin in the SERS studies. In addition, the UV-Vis spectrum of as prepared Ag NPs was measured with the aim of controlling the obtained Ag NPs before their use in the SERS substrate preparation.

SERS detection of 4−MBA in standard solutions: enhancement factor determination: A volume of 20.0 μL of each diluted solution of 4−MBA was dropped onto different 1 cm × 1 cm × 0.5 cm pieces of Ag NPs gel placed on microscope slides. Later, the gels were allowed to dehydrate at ambient temperature, protected from light, for about 24 h before the SERS measurements. A dehydrated gel with only 20.0 μL of ethanol was also examined as blank sample.

SERS detection of TBZ in standard solutions: calibration curves: A volume of 20.0 μL of each solution of TBZ was dropped onto different 1 cm × 1 cm × 0.5 cm pieces of Ag NPs gel placed on microscope slides. Subsequently, the gels were allowed to dehydrate as described above before SERS measurements. Dehydrated gels without any sample or with only 20.0 μL of methanol were also examined as blank samples.

In order to better understand the behaviour of the Ag NPs gel substrate, several factors were explored and analysed using TBZ as analyte. The expiration period of the substrate, the degree of dehydration, the ability to encapsulate the analyte and consequently to conserved it together with SERS Raman activity over time were among the factors highlighted to take into consideration. An improved knowledge of the SERS substrate allows optimizing the SERS signals, which enables to decrease the limit of detection, in this case, of TBZ.

Fruits and Vegetables peels contamination and micro-extraction procedures: To investigate the ability of the Ag NPs gel substrate and the proposed method to extract and detect the presence of traces of TBZ on fruits and vegetables surfaces, pieces of 1 cm^2 of their peels were intentionally contaminated with different amounts of TBZ. A volume of 20.0 or 25.0 μL of solutions of TBZ was poured on the peels surfaces, achieving surface concentrations from 5.0×10^4 to 4.0 ng/cm^2. Once the solvent was dried, a micro-extraction process was performed on each of the contaminated peels: first, 20.0 or 25.0 μL of methanol (the same volume used in the contamination step) were dropped on the fruit or vegetable surface in order to dissolve the pesticide that was absorbed or had penetrated the peel. Then, each peel surface was rubbed with a piece of 1 cm × 1 cm of the Ag NPs gel for ~ 15 s using the substrate as a stamp. Subsequently, the SERS substrates were placed on microscope slides and allowed to dehydrate at room temperature, protected from light, for about 24 h before SERS measurement. The whole procedure is illustrated in Fig. 1.

Blank controls of the fruit or vegetable peels were also performed. For that, 20.0 or 25.0 μL of methanol were poured on each washed peels surfaces. After drying, the same volume of methanol was dropped onto each surface and then each peel was rubbed with the SERS gel substrate. The blank peels SERS substrates were also placed on microscope slides and allowed to dehydrate before the SERS measurements as described above.

Re-extraction test was performed on an apple peel containing 0.40 μg/cm^2 (maximum surface concentration corresponding to the linear range of the calibration curve) with the aim of evaluating the recoveries of each extraction and the capacity of the proposed method to quantify the TBZ present on the surfaces. For that, 1 cm × 1 cm of apple peel was first contaminated with the mentioned amount of TBZ and later was subjected to several micro-extraction processes until no SERS signal was observed on the employed substrates.

2.4. UV-Vis, STEM microscopy and Raman instrumentation

A Shimadzu UV-2600 spectrometer (Shimadzu Corporation, Kyoto, Japan) equipped with a double beam was employed for the UV-Vis absorption spectra acquisition. All spectra were recorded in the 190−900 nm spectral range using 1 cm path length quartz cells. Methanol or water was used as reference. The cut-off values are 205 and 190 nm, for methanol and water, respectively.

The STEM images were collected using an SEM-FEI model SCIOS 2 instrument (Thermo Fisher Scientific, Waltham, Massachusetts, USA). An acceleration voltage of 30.0 kV was employed for collecting the Ag NPs images. A lower acceleration voltage, between 2.0 and 5.0 kV, was used when collecting the dehydrated SERS substrate images in order to

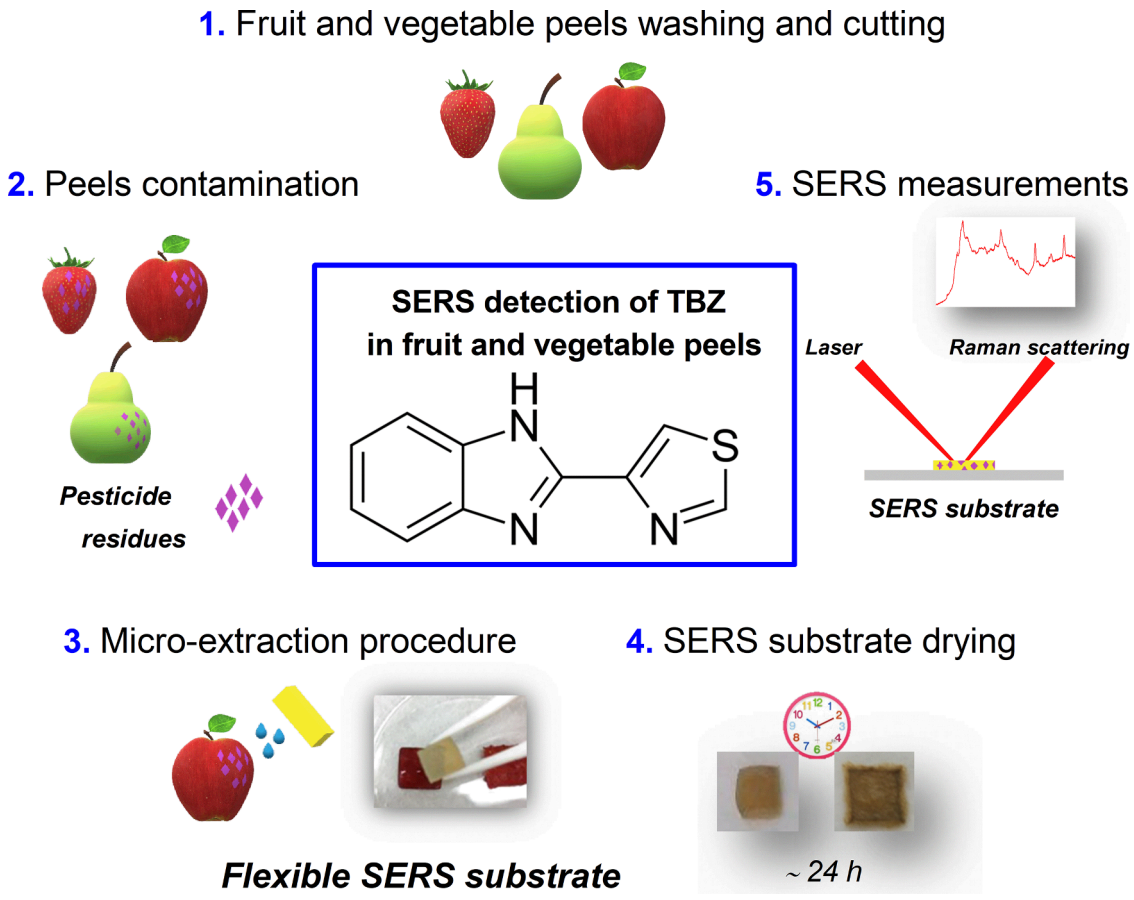

Fig. 1. Schematic representation of the experimental process.

prevent the surface from being charged even with metal coating.

Raman spectra were measured with a Horiba Jobin Yvon T64000 Raman spectrometer (Horiba, Villeneuve-d'Ascq, France) with a confocal microscope and equipped with CCD detector cooled with liquid nitrogen and a computer motorized XYZ mapping stage. The spectra were acquired in subtractive mode. Ar^+ and Kr^+ multiline lasers (Coherent Inc., Santa Clara, California, USA) were employed to provide the excitation source. The used lines were 476.5, 496.5 and 514.5 nm together with 647.1 and 676.4 nm wavelengths provided by the Ar^+ and Kr^+ lasers, respectively. The Raman wavenumbers calibration was performed using the band at 520.7 cm^{-1} of Si wafers (Merck, Darmstadt, Germany) or the band at 459.0 cm^{-1} of liquid CCl_4 (Cicarelli, Argentina) in a sealed glass capillary.

TBZ powder, pure methanol and a saturated methanol solution of TBZ (4.0×10^{-2} M) contained in sealed capillaries were measured using 10× objective (0.25 NA, Olympus Co., USA). On the other hand, 4−MBA power, pure acetone and concentrated acetone solution of 4−MBA (0.16 M) contained also in sealed capillaries were measured using 50× objective (0.75 NA, Olympus Co., USA). All samples were excited with a red laser of 647.1 nm wavelength (100 mW output power) provided by the Kr^+ multiline laser mentioned above. The laser power on the samples was ~ 3 and 1 mW for 10× and 50× objectives, respectively.

2.5. SERS measurements and data analysis

The SERS spectra were recorded with the previously described Raman instrument. Firstly, the wavelength of the excitation laser that maximizes the SERS signals for TBZ was investigated. For that, the SERS spectra of thiabendazole on the dehydrated Ag NPs gel substrate containing 4.0 μg/cm^2 were measured using a 50× objective (0.75 NA, Olympus Co., USA) and the above mentioned wavelength lines. After that, the samples were excited with the selected red laser of 647.1 nm wavelength using a 50× objective in order to focus the laser beam on the surface of the dehydrated substrates. The laser power on the samples was ~ 1 mW. For establish the uniformity of the SERS substrate and the SERS signal, typically, at least five spots on each surface were measured, while for a selected number of samples SERS mappings were also acquired. Typically, the SERS spectra were recorded with 10 s of acquisition time and 4 accumulations.

The analytical enhancement factor (AEF) was calculated for 4−MBA and TBZ by using the following expression [18]:

$$AEF = \frac{I_{SERS}/C_{SERS}}{I_{Raman}/C_{Raman}} \quad (1)$$

where, I_{SERS} is the intensity of a vibrational mode in the SERS spectrum, I_{Raman} is the intensity of the same mode in the Raman spectrum, C_{SERS} is the concentration of the analyte in the dehydrated Ag NPs gel substrate and C_{Raman} is the concentration of the analyte in the solution. To calculate the AEF the SERS and conventional Raman spectra were collected under identical experimental conditions (laser wavelength, laser power, microscope objective) and the spectra were normalized to acquisition time. The C_{SERS} was estimated considering than the hydrated gel shrinks its volume around 10 times after dehydration.

The LabSpec 5.45.09 software program was utilized to process all Raman spectra acquired. The analysis of the obtained SERS spectra provides information about the relationship between the Raman scattering intensity of a representative selected band of TBZ and the surface concentration of the fungicide on the substrate. The limit of detection (LOD) of TBZ was calculated using Eq. (2). [19]

$$LOD = \frac{3\ Sw}{b} \quad (2)$$

where, S_w corresponds to the standard deviation of the SERS intensity measured in the same wavenumber interval where the representative band of TBZ is integrated for a blank control, while b is the slope of the calibration curve in the linear region. Moreover, the recovery percentage was estimated whenever possible which allowed to analyze the feasibility of the proposed methods, as will be discuss in the next section.

2.6. DFT calculation

Density Functional Theory (DFT) calculations were performed with the Gaussian 03 program package [20]. The molecular structure of TBZ was optimized with the B3LYP/6-31+G(d) approximation by the simultaneous relaxation of all geometrical parameters. The vibrational IR and Raman spectra of the optimized structure were simulated using the same theoretical approximation.

3. Results and discussion

3.1. SERS substrate characterization

Fig. 2 shows the UV-Vis spectrum of the Ag NPs dispersion taken after their synthesis. The absorbance maximum was observed at 430 nm, as it was expected [13,15]. A STEM image of the obtained ~ 50 nm size particles is also shown in the figure together with a picture of the dispersion. Fig. 2 also presents some of the STEM images taken from the dehydrated Ag NPs gel after coating the sample with gold as mentioned above. The Ag NPs seems to be homogeneously distributed in the gel substrate. Considering that the diameter of the incident laser spot size at the sample is ~ 1 μm, it can be concluded from the images that there will be a large number of nanoparticles (potentially hot spots) in each spot.

3.2. Evaluation of relevant experimental parameters for TBZ

As mentioned before, the presence of resonance or pre-resonance Raman effects were explored. For that, UV-Vis spectra of TBZ in methanol solutions were obtained before starting the Raman measurements.

TBZ UV-Vis spectra: Fig. S1 of the Supplementary Information shows the UV-Vis spectra of TBZ in methanol solutions of different concentration. The spectrum showed strong absorptions at 206, 235, 242 and 299 nm wavelength. The absorption presents at higher wavelength has been previously reported in chloroform at 302 nm [21]. Recently, the simulated spectrum was also reported and interpreted in terms of electronic transitions through NBO analysis [22]. The UV-Vis spectrum suggested that pre-resonance or resonance Raman effects are not expected when visible lasers are used to provide the excitation source.

Excitation wavelength selection: Although no resonance or pre-resonance Raman effects are expected for this sample excited with visible lasers, SERS spectra were collected with different excitation wavelengths in order to optimize the experimental conditions aiming SERS analytical applications. Dehydrated Ag NPs gel substrate containing 4.0 μg/cm^2 was explored using the laser wavelengths previously mentioned. The maxima SERS signals were obtained with 647.1 and 676.4 nm wavelengths provided by a Kr^+ multiline laser. Finally, the line at 647.1 nm wavelength was chosen for being the most intense one.

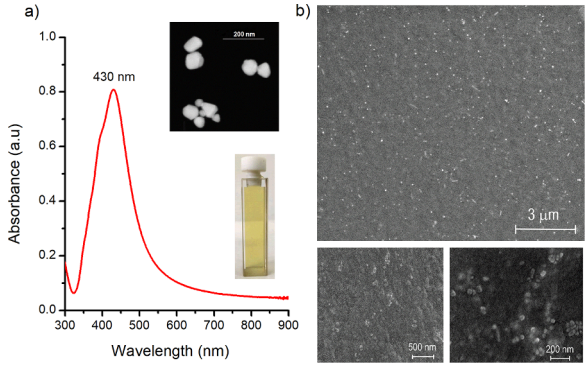

Fig. 2. (a) UV-Vis absorption spectrum of 1:10 dilution with Milli-Q water of the Ag NPs dispersion taken after being synthetized. A STEM image of the nanoparticles is shown in the inset together with a photograph of the diluted dispersion, (b) STEM images of 10 nm gold-coated dehydrated Ag NPs gel substrate.

Ag NPs gel substrate background spectrum: Fig. S2 of the Supplementary Information shows the blank spectrum of dehydrated Ag NPs gel substrate where only 20.0 μL of the solvent methanol were poured on the surface before dehydration. The spectrum shows a clean spectral window in the ~250−3500 cm^{-1} region, consistent only of the low cross-section Raman signals of polysaccharides [23]. The intense band sometimes observed at 225 cm^{-1} can be attributed to Ag−O vibrational mode [24]. Normally, the intensity of this band increases when the substrate is exposed to the air and/or laser radiation.

3.3. SERS substrate performance: AEF for 4−MBA

Fig. S3 shows conventional Raman spectra of solid 4−MBA and of a 0.16 M acetone solution and SERS spectrum of 4−MBA taken with the 647.1 nm excitation line and the 50× objective. As reported before [17], the band at 2564 cm^{-1} in the solid Raman spectrum, assigned to the S−H stretching mode, disappears after the 4−MBA molecules are absorbed into the metal, evidencing a dissociative adsorption of the S−H group. The bands present at 1594 and ~1097 cm^{-1} in the concentrated solution were chosen to estimate the AEF, both related to aromatic ring vibrational modes [17]. These two bands are shifted in the SERS spectrum and appear at 1583 and 1074 cm^{-1}, respectively. It is well known than the enhanced factor depends on many different parameters as excitation wavelength, vibrational mode, molecular adsorption geometry, between others [18]. In this study, the AEF for the above mention vibrational modes were determined employing a SERS spectrum of an intermediate 4−MBA concentration. Fig. S4 presents SERS representative spectra obtained for 4−MBA on Ag NPs gels varying the amount of analyte on the substrate. The substrate loaded with 20.0 μL of 4−MBA ethanol solution 1.0×10^{-4} M was chosen to determine the AEF and therefore spectra at different spots on the substrate were collected (Fig. S5) to calculate an average integrated area for the selected bands. The AEF for 4−MBA of ~10^6 was obtained for both selected bands (AEF_{1074} ~ 7×10^5; AEF_{1583} ~ 2×10^6).

3.4. Raman and SERS measurements of TBZ

Raman and SERS spectra of TBZ: Fig. 3 shows conventional Raman and SERS spectra of TBZ taken with the 647.1 nm excitation line. The former corresponds to the spectrum of a solid sample of TBZ sealed in a glass capillary while the SERS spectrum was measured from a Ag NPs gel substrate containing ~ 2 μg/cm^2 of TBZ. In addition, Fig. S6 of the Supplementary Information presents the conventional Raman spectrum of a TBZ saturated methanol solution, together with the spectrum of pure methanol. The spectrum of the solution is completely dominated by the methanol bands, which overlap the most intense signals of TBZ, which are practically in the same positions than in the solid phase. Nevertheless, the Raman band at 779 cm^{-1} in methanol solution was chosen to estimate the AEF for TBZ, taking into account the same assumptions made for 4−MBA. The AEF estimated using the SERS spectrum loaded with 20.0 μL of TBZ methanol solution 7.5×10^{-5} M was ~ 7×10^6. The most important bands of TBZ in solid phase and in methanolic solution are summarized in the Supplementary Information (Table S1) together with their tentative assignment. Fig. S7 of the Supplementary Information presents the atom numbering refereed in the assignment. TBZ structure presents a benzimidazole and a thiazole moieties. Likewise, the benzimidazole moiety consists of phenyl and imidazole rings (Fig. S7).

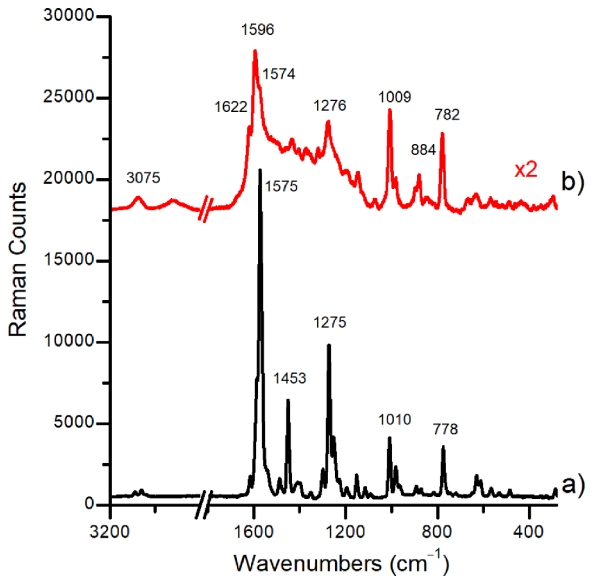

Fig. 3. (a) Raman spectrum of thiabendazole powder sample (excitation wavelength: 647.1 nm; laser power 200 mW; acquisition time: 10 s; 4 accumulations; 10x objective (0.25NA)), (b) SERS spectrum of thiabendazole on the Ag NPs gel substrate containing ~ 2 μg/cm^2 of thiabendazole (Excitation wavelength: 647.1 nm; laser power: 100 mW; acquisition time: 10 s; 8 accumulations; 50× objective (0.75NA)).

There are several reports about Raman and SERS spectra of TBZ in the literature together with proposed vibrational assignment [22,25,26]. The tentative assignment presented in this study (Table S1) was performed not only by comparing the reported ones in the literature but also taking into consideration the simulated spectrum calculated using the B3LYP/6-31+G(d) approximation. The most significant changes in the SERS spectrum of TBZ in comparison with that of the solid phase are the intensity enhancement of the bands corresponding to C−H stretching modes (broadband at ~3075 cm^{-1}), the signal at ~884 cm^{-1}, that can be attributed to the symmetric CSC stretching mode (ν_s (CSC)) of the thiazole moiety, and the bands at 782 and 1009 cm^{-1}, assigned to the ν_{as} (CSC) and νC−C of the phenyl group, respectively. Another difference between the Raman spectrum of the solid sample and the SERS spectra is observed in the spectral region between 1700 and 1276 cm^{-1}, which corresponds to several modes involving CN stretching vibrations. This spectral region of the SERS spectra is characterized by superposed signals with fluctuating relative intensities. These changes can be related to different orientations of the molecule onto the metallic surface [27]. Taking into account the molecular structure of TBZ, the molecules could be adsorbed through a lone electron pair of N or of S atoms (or both), resulting in a standing-up orientation to the Ag NPs surface, or through the π ring electrons, deriving in a parallel orientation to the surface [25–27]. The fact that the most enhanced modes correspond to stretching vibrations, together with the strong presence of the bands assigned to the thiazole moiety in the SERS spectrum, supports the proposal of an interaction thought the thiazole ring resulting in a stand-up orientation of the molecule to the metallic surface. Recently, Oliveira et al. [27] proposed, based on local reactivity DFT calculations, that the most plausible interaction between the thiazole moiety and the Ag NPs surface is *via* the S atom.

SERS detection of TBZ in standard solutions: Calibration curves: Prior to assessing the detection of the title fungicide in fruit and vegetable peels, the analysis of the spectra collected varying the surface concentration of TBZ directly on the substrate was performed. Fig. 4a shows selected SERS spectra of TBZ on Ag NPs gel substrates measured after dehydration. As discussed in the previous section, the relative intensities of some

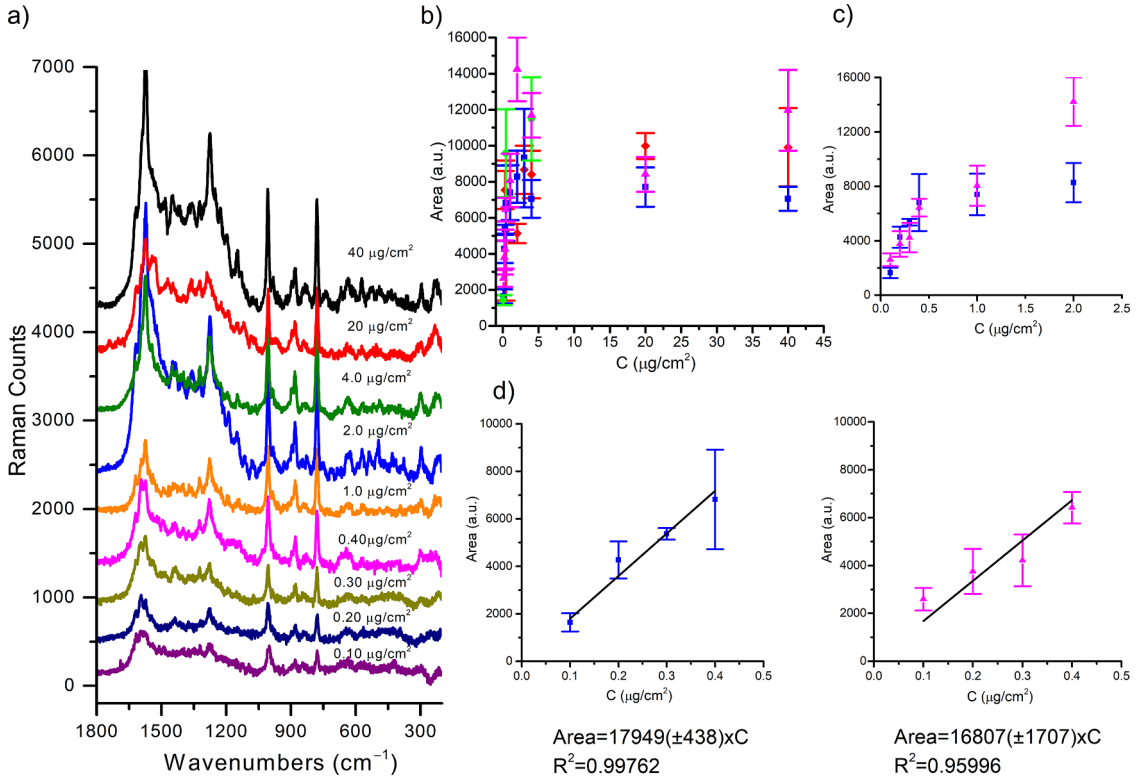

Fig. 4. (a) SERS representative spectra of thiabendazole on AgNPs gel substrate at different concentrations. (b) Thiabendazole SERS intensity measured at 782 cm^{-1} (peak area integrated between 801 and 762 cm^{-1}) as a function of thiabendazole concentration in μg/cm^2. Each symbol corresponds to a different batch of employed substrate. Furthermore, each point corresponds to an average of at least five different spots and error bars indicated S. D. (c) Selected region of the graph (b) where only the most completed calibration curves are shown. (d) Fitting of the linear region of these calibration curves.

Raman bands appear to change in the SERS spectra not only with the TBZ surface concentration but also with the measured spot. Moreover, fluctuations in the intensity of several bands were also observed during the laser exposition time, mainly in the region comprised between 1276 and 1700 cm^{-1}. Nevertheless, the bands present at 1009 and 782 cm^{-1} remained stable during the laser exposition and did not show a significant change between the spectra randomly collected. For these reasons, these signals were firstly chosen to explore the possibility to perform a quantitative or semi-quantitative analysis. On the other hand, the substrate background presents a low-intensity band at 1000 cm^{-1} that difficult the measurement of the area of the 1009 cm^{-1} signal, especially in the low concentration samples. Therefore, the band located at 782 cm^{-1} was finally selected to perform the analyses. Fig. 4b shows the dependence of the SERS intensity against the TBZ concentration measured using different batches of substrates prepared on different days. Each point in the plot corresponds to an average intensity of five randomly collected spots, and the standard deviation (S. D.) for each point is indicated as error bar. Since the SERS intensity is proportional to the number of molecules adsorbed at the substrate, the plot presented in Fig. 4b can be considered as an adsorption isotherm [28]. As can be noted in the figure, the shown isotherms present the same behavior although there is a variation in the SERS intensity values depending on the Ag NPs gel substrate batch and the day when the spectra were collected. In the literature it has been accepted that the S. D. value from substrate-to-substrate (different batches for instance) and from spot-to-spot should be less than 20% [29], condition that is achieved in the experiments presented in this work.

At low concentrations of TBZ (0.10 to 0.40 $\mu g/cm^2$), the intensity of the SERS signals increases linearly with the concentration, as shown in Fig. 4c. At higher concentrations, the intensity of the SERS bands increases and achieves saturation at $\sim$ 2 $\mu g/cm^2$. Nevertheless, the SERS intensity decreases when the surface concentration of TBZ is higher than $\sim$ 5 $\mu g/cm^2$, suggesting intermolecular interactions between the adsorbed molecules. Fig. 4d shows the linear behavior observed at lower concentration for two different substrate batches; this interval can be used for quantitative or semi-quantitative analytical approaches. The fitting of the linear region of these calibration curves are also shown in the Figure. After analyzing the performance of the Ag NPs gel substrates for quantitative or semi-quantitative analysis, the determination of the calibration curve together with the measurement of the unknown sample using the same batch of flexible SERS substrate should be recommended. On the other hand, this is not necessary if the SERS substrate will be employed only as a *presence-absence test*. In addition, the LOD of TBZ was calculated using the Eq. (2). The obtained value for both calibration curves shown in Fig. 4d was 30 ng/cm^2.

Features of Ag NPs gel substrates and TBZ: For the sake of better understanding of the behavior of the Ag NPs gel substrates for the determination of TBZ by SERS, a series of experiments were realized. Firstly, as mention above, the *SERS spectrum* appears to change not only from spot-to-spot but also with the surface concentration of TBZ. Fig. 5 presents the SERS spectra of dehydrated Ag NPs gel substrates containing 4.0 or 0.40 $\mu g/cm^2$ of TBZ, collected at ten different spots each. For both concentrations, changes in the spectrum were observed mostly in the spectral region comprised between 1276 and 1700 cm^{-1}. These variations might be related to different molecular orientations [30,31] that can change with either the surface concentration of TBZ or the adsorption site on the substrate. In addition, the laser heating effects can also affect the orientation of the adsorbed molecules leading to the fluctuations observed during the spectra measurement.

As mention before, the signal at 782 cm^{-1} remained almost invariable in all randomly collected spectra of Ag NPs gel substrate with certain TBZ loading. This fact can be seen either in Fig. 5 for two different TBZ loading of the substrate or in the map shown in Fig. 6. The 60 $\times$ 60 μm area map of Ag NPs gel substrate containing 0.40 $\mu g/cm^2$ was collected in order to additionally evaluate the *uniformity of the substrate*. The histogram representation for the 121 spots of the map was fitted by a normal distribution function. The uniformity of the TBZ signal at 782 cm^{-1} on the substrate, as it can be seen in the SERS mapping, would allow a straight and fast determination taken only a small number of spots.

The *SERS performance* of the substrate is also affected by the *hydration degree* of the substrate that contains the analyte. There is a substantial increase of the SERS signal as the gel loses water until it dehydration. To exemplify this fact, Fig. S8 of the Supplementary Information shows selected spectra of TBZ on the Ag NPs gel substrate containing 4.0 $\mu g/cm^2$ before and after dehydration. This observation can be easily interpreted in terms of electromagnetic coupling between two or more metallic nanoparticles, which produces a redshift of the corresponding localized surface plasmon resonance (LSPR) allowing for an overlap between the LSPR and the laser line employed. Therefore, the gel collapses upon drying and acts as a molecular trap promoting dynamic hot spots (D-SERS), as has been reported and explained in the literature [23]. The trapped molecules are homogenously distributed into the dehydrated gel, at least when the TBZ surface concentration is higher than 0.10 $\mu g/cm^2$. Furthermore, the SERS intensity does not depend on the *side of the substrate*, namely, once the analyte is trapped the spectrum can be collected from the surface which was in contact with the sample or from the other side, indistinctly. Fig. S9 of the Supplementary Information shows selected SERS spectra of TBZ on Ag NPs gel substrate containing 2 $\mu g/cm^2$ collected from both sides of the substrate: top and down.

In addition, a selected dehydrated Ag NPs substrate containing 2 $\mu g/cm^2$ of TBZ was conserved at ambient temperatures, protected from light, and periodically measured to evaluate its ability to *conserve the trapped analyte*. Selected spectra are presented in the Supplementary Information (Fig. S10). The SERS signals were observed, with almost equal intensity, for at least 22 months after being prepared. The ability to conserve the trapped molecules and its long-term SERS activity were also observed for others analytes: cocaine [14] and thiram [13].

Finally, the *expiration time* of the Ag NPs gel substrate was investigated. After its preparation, the gel substrate is storage in the fridge until being used; this is approximately within 10 days of being prepared, as it was mentioned in a previous reported work [13,32]. Fig. S11 of the Supplementary Information shows selected SERS spectra of Ag NPs gel

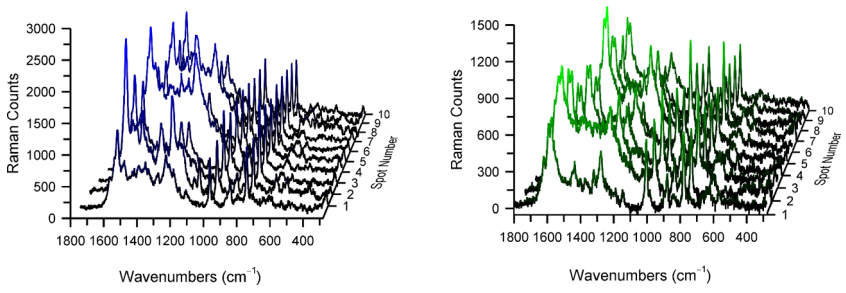

Fig. 5. SERS spectra of Ag NPs gel substrates containing 4.0 $\mu g/cm^2$ (left) and 0.40 $\mu g/cm^2$ (right) of thiabendazole. (Excitation wavelength: 647.1 nm; laser power: 100 mW; acquisition time: 10 s; 4 accumulations; 50$\times$ objective (0.75NA)).

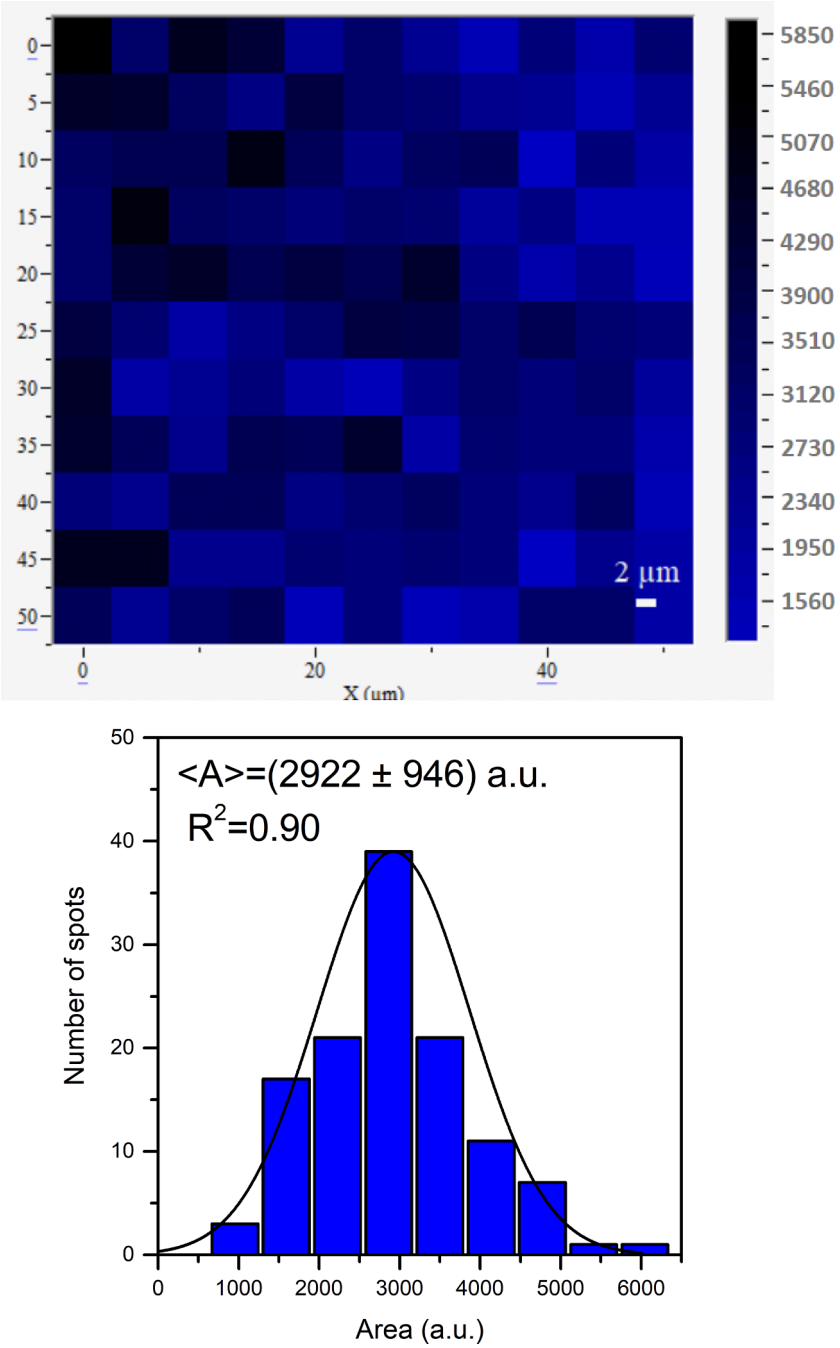

Fig. 6. Left: SERS mapping (60 × 60 µm, step size 5 µm) of Ag NPs gel substrate containing 0.40 µg/cm^2 of thiabendazole. The peak area was integrated between 801 and 762 cm^{-1}. Right: Intensity histograms together with its Gaussian fit. Excitation wavelength: 647.1 nm; laser power: 100 mW; acquisition time: 10 s; 2 accumulations; 50× objective (0.75NA)).

substrates of different ages, all of them containing the same amount of TBZ (4.0 µg/cm^2). As the age of the substrate increases, the SERS response decreases. This might be due to the fact that in the fridge the gel starts to dehydrate and after that the substrate losses its role of molecular trap compromising its SERS activity. So, to obtain better SERS results, it is recommended to use the substrate within the 10 days after its preparation. This drawback can be compensated by the great stability of the Ag NPs dispersion and the simple and fast substrate preparation, resulting of great importance for practical applications.

3.5. TBZ detection on various fruit and vegetable peels

The Ag NPs gel substrate was employed for the *in-situ* detection of TBZ residues in various fruit and vegetable peels. The spectra of the blank control experiments, presented as Supplementary Information, showed no obvious signals (Fig. S12). An exception for that was the green pepper that showed several bands that are compatible with the presence of TBZ in low surface concentration. The blank Raman spectra of pear peels also showed the presence of TBZ in one of the pears used in this work. Fig. S13 of the Supplementary Information presents the blank Raman spectra obtained from pears bought in different stores. One of them showed no obvious signals; however, in another the fungicide TBZ was present as mentioned before. Finally, as it can be seen in the Figure, one pear peel presented a reproducible SERS spectrum that could not be identified. Moreover, clean green pepper and pear peels with no obvious SERS signals were employed in the experiments performed to investigate

the ability of the Ag NPs gel substrate to extract and detect the presence of TBZ. Fig. 7 shows selected spectra of the dehydrated substrates employed to extract the fungicide from vegetable and fruit peels (eggplant, green pepper, tomato, strawberry, apple and pear) contaminated with different dosage of TBZ. As can be seen in the Figure, for eggplant and green pepper 0.050 μg/cm^2 was the lowest value of TBZ that could be detected with this method. On the other hand, the lowest TBZ surface concentration that could be identified in tomato and strawberry peels was 0.50 μg/cm^2, while the value for apple and pear were 0.20 and 0.040 μg/cm^2, respectively.

In order to determine the recovery of the TBZ from the fruit or vegetable surface rubbed or stamped with the SERS substrate, the extracted quantities were determined using the calibration curves, but only for intensity areas included in the linear zone (intensity area between ~7000 and 2000 a.u., depending on the calibration curve used). The recoveries were estimated comparing the surface concentration spiked on the peels with the obtained values after measuring the intensity area of the 782 cm^{-1} band and using the calibration curves. The highest estimated recoveries were obtained for green pepper and eggplant, ~100% of the fungicide was recovered from there surface peels during the first extraction. For pear, tomato and apple, the estimated recoveries were comparable, being ~60–50% for all of them. The lowest recovery value was obtained for strawberry, only ~ 12% of TBZ could be recovered from the surface with the proposed method. The variation in sensitivity and the degree of TBZ recoveries are attributed to differences in surface properties of vegetable and fruit peels that affect both the TBZ penetration into the inner of the peel and the interaction strength between the peels and TBZ. These differences are responsible of the diverse lowest values of TBZ detected in the different vegetable and fruit peels.

Additionally, Fig. 8 shows selected SERS spectra obtained for successive extraction performed on an apple peel containing initially 0.40 μg/cm^2. After the first extraction, the TBZ recovered from the peel was ~ 60%, leaving a surface concentration of ~ 0.16 μg/cm^2. Then, a second micro-extraction was performed on the apple peel and the analyte recovered was ~ 70% that leaves a surface concentration of ~ 0.050 μg/cm^2. Finally, in a third micro-extraction no SERS signal was observed, in accordance with lowest TBZ surface concentration expected for TBZ for

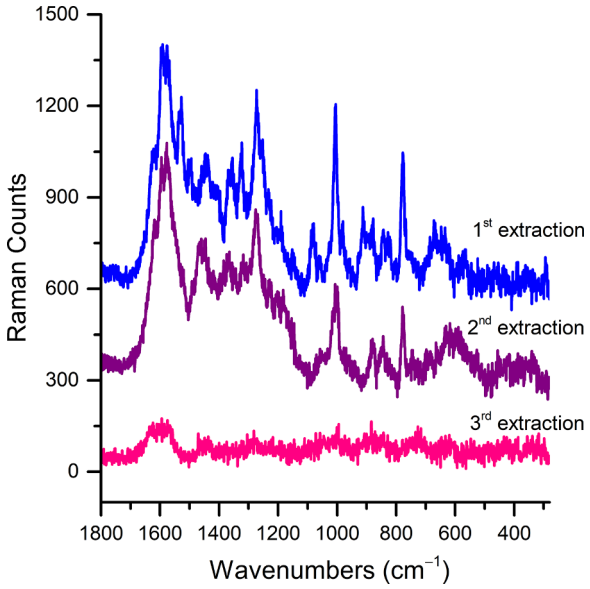

Fig. 8. Selected SERS spectra of Ag NPs gel substrates rubbed over an apple peel initially containing 0.40 μg/cm^2 of thiabendazole. (Excitation wavelength: 647.1 nm; laser power: 100 mW; acquisition time: 10 s; 4 accumulations; 50× objective (0.75NA)).

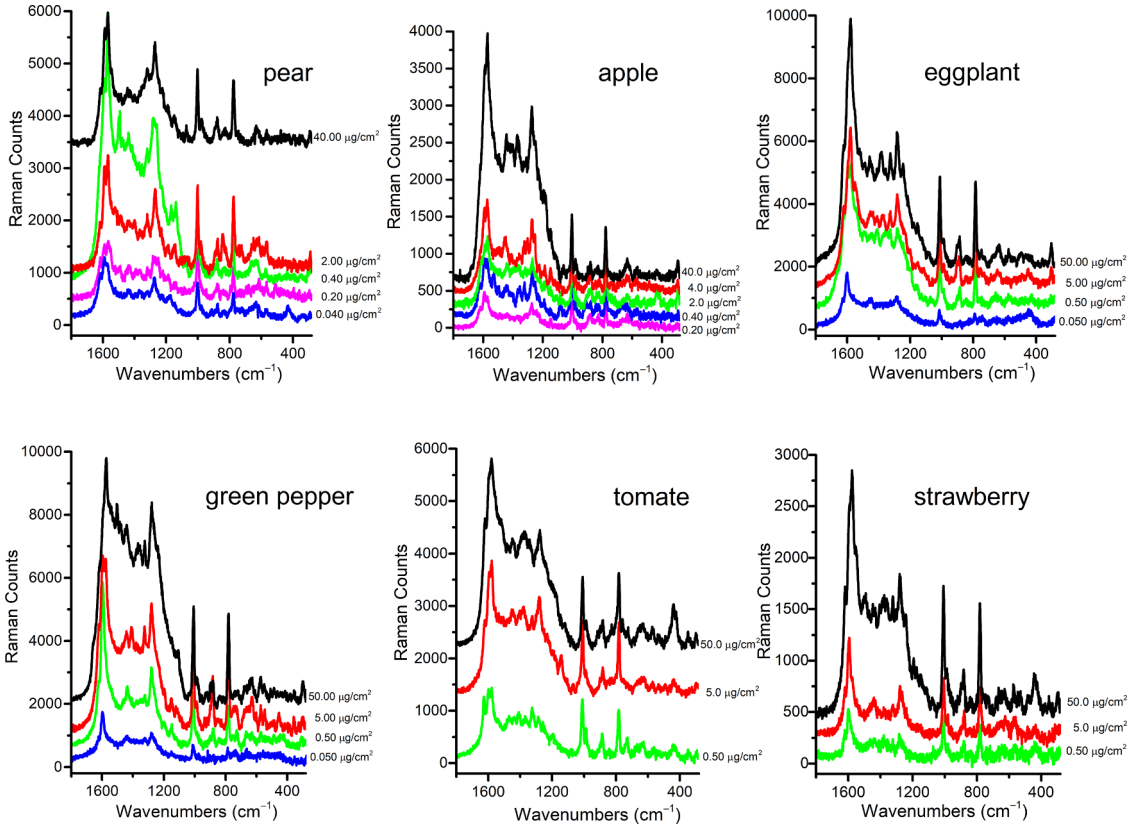

Fig. 7. Selected SERS spectra of Ag NPs gel substrates rubbed over different vegetable and fruit peels contaminated with thiabendazole. (Excitation wavelength: 647.1 nm; laser power: 100 mW; acquisition time: 10 s; 4 accumulations; 50× objective (0.75NA)).

apple peel (0.20 μg/cm^2).

The minimum concentration (in ppm) that can be detected for apples with the proposed method can be estimated making few considerations. On one hand, considering a spherical shaped apple of ~ 8 cm of diameter (see apple sizing reference [32]) and that the pesticide is only present in the apple peel, then the total amount of TBZ that could be detected with this method is ~ 40 μg (0.20 μg/cm^2 × 200 cm^2). On the other hand, considering the weight of the apple around 220 g, the estimated minimum concentration (in ppm) detected is ~ 0.2 ppm. This allows us to compare the minimum surface concentration detected with the MRL values established for governmental agencies being the MRL one order of magnitude higher than the detected with this methodology.

Taking into account the simplicity of the proposed method and the excellent SERS performance of the substrate, together with their ability to encapsulate and to conserve the analyte and to make it available for future measurements, this flexible SERS substrate results in a promising platform for food safety applications enabling *in-situ* inspection and trace detection of harmful chemical residues. In addition, the flexibility of the substrate is a very important and remarkable characteristic of the substrate presented in this work, since it can easily adapt to the surface of the fruit or vegetable for the analyte extraction.

In summary, the flexible SERS substrates based on silver nanoparticles immersed in an agar gel reaches a limit of detection of 30 ng/cm^2 (~ 9×10^5 molecules/spot, 0.3 fg/spot) for thiabendazole. The proposed method is suitable for the detection of TBZ in fruit and vegetable peels and allows *on-site* inspection of its presence under the limits established by the governmental agencies. Lastly, Table S2 of the Supplementary Information shows a comparison of the performance of different reported SERS substrates for TBZ detection on various fruit or vegetable peels. As can be seen in the Table, the method described in this work shows notable LOD on the fruit and vegetables peels investigated, especially when the obtained limits are compared with the reported ones.

CRediT authorship contribution statement

María Luz Rizzato: Investigation, Formal analysis. **A. Lorena Picone:** Conceptualization, Writing – original draft, Writing – review & editing, Investigation, Formal analysis. **Rosana M. Romano:** Conceptualization, Writing – original draft, Writing – review & editing, Funding acquisition.

Declaration of Competing Interest

The authors declare that they have no known competing financial interests or personal relationships that could have appeared to influence the work reported in this paper.

Data availability

Data will be made available on request.

Acknowledgment

We would like to deeply thank the fruitful discussions with Prof. Dr. Dr. Carlos O. Della Védova. We also thank Ing. Matías Calderón, Lic. Gustavo Pozzi and Gino Pietrodangelo for their help during the Raman measurements. The STEM images have been possible thanks to the work of Lic. María Alejandra Floridia Addato under the supervision of Dr. Alberto Caneiro (YTEC-CONICET). We are grateful to Dr. Antonieta Daza Millone for providing us with the 4−MBA reagent. Finally, we are grateful to the technicians of CEQUINOR who have also collaborated to the present work.

Funding sources

This work was supported by Facultad de Ciencias Exactas of Universidad Nacional de La Plata (UNLP-11/X822), Consejo Nacional de Investigaciones Científicas y Tecnológicas CONICET (PIP 0352) and Agencia Nacional de Promoción Científica y Tecnológica ANPCyT (PICT-2017-2034).

Supplementary materials

Supplementary material associated with this article can be found, in the online version, at doi:10.1016/j.talo.2023.100223.

References

[1] United States Environmental Agency (U.S. EPA). Prevention, pesticides and toxic substances. Thiabendazole. Retrieved from https://www3.epa.gov/pesticides/chem_search/reg_actions/reregistration/red_PC-060101_1-May-02.pdf. Accessed October 2022.
[2] United States Environmental Agency (U.S. EPA). Pesticide tolerances. Retrieved from https://www.epa.gov/pesticide-tolerances/how-search-tolerances-pesticide-ingredients-code-federal-regulations. Accessed October 2022.
[3] SENASA. Resolución-934-2010. Servicio Nacional de Sanidad y Calidad Agroalimentaria. Retrieved from http://www.senasa.gob.ar/normativas/resolucion-934-2010-senasa-servicio-nacional-de-sanidad-y-calidad-agroalimentaria. Accessed October 2022.
[4] European Commission, 2022, Maximum residue levels. Retrieved from https://food.ec.europa.eu/plants/pesticides/eu-pesticides-database_en. Accessed October 2022.
[5] M.L. Xu, Y. Gao, X.X. Han, Innovative application of SERS in food quality and safety: a brief review of recent trends, Foods 11 (2022) 1–12, 2097.
[6] C. Liu, D. Xu, X. Dong, Q. Huang, A review: research progress of SERS-based sensors for agricultural applications, Trends Food Sci. Technol. 128 (2022) 90–101.
[7] A. Nilghaz, S.M. Mousavi, A. Amiri, J. Tian, R. Cao, X. Wang, Surface-Enhanced Raman Spectroscopy substrates for food safety and quality analysis, J. Agric. Food Chem. 70 (2022) 5463–5476.
[8] D. Zhang, H. Pu, L. Huang, D.W. Sun, Advances in flexible surface-enhanced Raman scattering (SERS) substrates for nondestructive food detection: Fundamentals and recent applications, Trends Food Sci. Technol. 109 (2021) 690–701.
[9] R. Li, M. Chen, H. Yang, N. Hao, Q. Liu, M. Peng, L. Wang, Y. Hu, X. Chen, Simultaneous *in situ* extraction and self-assembly of plasmonic colloidal gold superparticles for SERS detection of organochlorine pesticides in water, Anal. Chem. 93 (2021) 4657–4665.
[10] R. Li, Z. Wang, Z. Zhang, X. Sun, Y. Hu, H. Wang, K. Chen, Q. Liu, M. Chen, X. Chen, Deep learning-based multicapturer SERS platform on plasmonic nanocube metasurfaces for multiplex detection of organophosphorus pesticides in environmental water, Anal. Chem. 94 (2022) 16006–16014.
[11] S. Wang, Q. Hao, Y. Zhao, Y. Chen, Two-dimensional printed AgNPs@ paper swab for SERS screening of pesticide residues on apples and pears, J. Agric. Food Chem. 71 (2023) 4982–4989.
[12] X. Dai, D. Danni Xue, X. Liu, C. Gu, T. Jiang, An adhesive SERS substrate based on a stretched silver nanowire-tape for the *in situ* multicomponent analysis of pesticide residues, Anal. Methods 15 (2023) 1261–1273.
[13] A.L. Picone, M.L. Rizzato, A.R. Lusi, R.M. Romano, Stamplike flexible SERS substrate for *in-situ* rapid detection of thiram residues in fruits and vegetables, Food Chem. 373 (2022), 131570, 1-8.
[14] A.L. Picone, C.O. Della Védova, R.M. Romano, Study on the detection of cocaine in Argentinean banknotes by SERS, Vib. Spectrosc. 373 (2020), 131579, 1-8.
[15] O.S. Isanova, F.P. Zamborini, Size-dependent electrochemical oxidation of silver nanoparticles, J. Am. Chem. Soc. 132 (1) (2010) 70–72.
[16] E. Platania, C. Lofrumento, E. Lottini, E. Azzaro, M. Ricci, M. Becucci, Tailored micro-extraction method for Raman/SERS detection of indigoids in ancient textiles, Anal. Bional. Chem. 407 (2015) 6505–6514.
[17] A. Michota, J. Bukowska, Surface-enhanced Raman scattering (SERS) of 4-mercaptobenzoic acid on silver and gold substrates, J. Raman Spectr. 34 (2003) 21–25.
[18] y E.C. Le Ru, E. Blackie, M. Meyer, P.G. Etchegoin, Surface enhanced Raman scattering enhancement factors: a comprehensive study, J. Phys. Chem. C 111 (2007) 13794–13803.
[19] N. Hussain, H. Pu, D.W. Sun, Core size optimized silver coated gold nanoparticles for rapid screening of tricyclazole and thiram residues in pear extracts using SERS, Food Chem. 350 (2021), 129025, 1-11.
[20] M.J. Frisch, G.W. Trucks, H.B. Schlegel, G.E. Scuseria, M.A. Robb, J.R. Cheeseman, Jr.J.A. Montgomery, T. Vreven, K.N. Kudin, J.C. Burant, et al., Gaussian 03; Rev. B.04, Gaussian, Inc., Pittsburgh, PA, 2003.
[21] A. Raizman, Determination of thiabendazole in citrus fruis by ultraviolet spectrophotometry, Analyst 99 (1974) 120–127.
[22] A.M. Tabanez, B.A. Nogueira, A. Milani, M.E.S. Eusebio, Paixão, H.N. Kabuk, M. Jajuga, G.O. Iliz, F Rui, Thiabendazole and thiabendazole-formic acid solvate: a computational, crystallographic, spectroscopic and thermal study, Molecules 25 (2020) 3093, 1-26.

[23] P. Aldeanueva-Potel, E. Faoucher, R.A. Alvarez-Puebla, L.M. Liz-Marzán, M. Brust, Recyclable molecular trapping and SERS detection in silver-loaded agarose gels with dynamic hot spots, Anal. Chem. 81 (2009) 9233–9238.
[24] P.S. Mdluli, N.M. Sosibo, N. Revaprasadu, P. Karamanis, J. Leszczynski, Surface enhanced Raman spectroscopy (SERS) and density functional theory (DFT) study for understanding the regioselective adsorption of pyrrolidinone on the Surface of silver and gold colloids, J. Mol. Struct. 935 (2009) 32–38.
[25] M.S. Kim, M.K. Kim, C.J. Lee, Y.M. Jung, M.S. Lee, Surface-enhanced Raman spectroscopy of benzimidazolic fungicides: benzimidazole and thiabendazole, Bull. Korean Chem. Soc. 30 (2009) 2930–2943.
[26] C. Müller, L. David, V. Chiş, S.C. Pînzaru, Detection of thiabendazole applied on citrus fruits and bananas using surface enhanced Raman scattering, Food Chem. 145 (2014) 814–820.
[27] M.J.S. Oliveira, R.J.G. Rubira, L.N. Furini, A. Batagin-Neto, C.J.L. Constantino, Detection of thiabendazole fungicide/parasiticide by SERS: Quantitative analysis and adsorption mechanism, Appl. Surf. Sci. 517 (2020), 145786, 1–8.
[28] K.V. De Oliveira, J.C. Rubim, Surface-enhanced Raman spectroscopy of molecules adsorbed on silver nanoparticles dispersed an agarose gel and their adsorption isotherms, Vib. Spectrosc. 86 (2016) 290–301.
[29] K. Wang, D.W. Sun, H. Pu, Q. Wei, Two-dimensional Au@Ag nanodot array for sensing dual-fungicides in fruit juices with surface-enhanced Raman spectroscopy technique, Food Chem. 310 (2020) 1–20.
[30] B. Fortuni, Y. Fujita, M. Ricci, T. Inose, R. Aubert, G. Lu, J.A. Hutchison, J. Hofkens, L Latterini, H. Uji-I, A novel method for *in-situ* synthesis of SERS-active gold nanostars on polydimethylsiloxane film, Chem. Commun. 53 (2017) 5121–5124.
[31] H. Luo, Y. Huang, K. Lai, B.A. Rasco, Y. Fan, Surface-enhanced Raman spectroscopy coupled with gold nanoparticles for rapid detection of phosmet and thiabendazole residues in apples, Food Control 68 (2016) 229–235.
[32] The size of stemilt apple. Retrieved from http://www.stemilt.com/assets/pdfs/AppleSizing.pdf. Accesed October 2022.